

Chemically regenerative redox fuel cells

D-G. OEI

Engineering and Research Staff, Ford Motor Company, Dearborn, Michigan 48121, USA

Received 26 March 1981

Exploratory experiments with three types of redox fuel cells utilizing the $\text{VO}_2^+/\text{VO}^{2+}-\text{Sn}^{2+}/\text{Sn}^{4+}$, $\text{VO}_2^+/\text{VO}^{2+}-\text{Fe}^{2+}/\text{Fe}^{3+}$ and $\text{VO}_2^+/\text{VO}^{2+}-\text{Cu}/\text{Cu}^{2+}$ redox couples are reported. The results show the major features and problems, and suggest possible solutions to some of the problems associated with operating redox fuel cells. In this phase of experimentation the best individual cell performances that were achieved showed that the $\text{VO}_2^+/\text{VO}^{2+}-\text{Sn}^{2+}/\text{Sn}^{4+}$ redox cell had a power density of 0.049 W cm^{-2} , the $\text{VO}_2^+/\text{VO}^{2+}-\text{Fe}^{2+}/\text{Fe}^{3+}$ redox cell had a power density equal to 0.049 W cm^{-2} and the $\text{VO}_2^+/\text{VO}^{2+}-\text{Cu}/\text{Cu}^{2+}$ redox fuel cell had a power density of 0.093 W cm^{-2} .

1. Introduction

The idea of a direct hydrogen-oxygen fuel cell, in which hydrogen and oxygen react electrochemically at the electrodes to generate electricity, was conceived in 1839 by Grove [1]. A major impetus toward the development of fuel cells was the thermodynamic analysis of fuel cell systems by Ostwald, Nernst and Haber amongst others, showing that this electrochemical energy conversion device was not Carnot limited and that its thermal efficiency was inherently higher than for the heat engine [2]. It was Nernst [3] who professed serious doubt about the easy adoption of Ostwald's idea of building a direct hydrogen-oxygen fuel cell and he subsequently proposed an indirect hydrogen-oxygen fuel cell or redox fuel cell. In the redox fuel cell the hydrogen and oxygen react indirectly using a redox couple as intermediary. The redox couple reacts electrochemically at the electrode, thus providing a source or a sink of electrons, and the hydrogen and oxygen are then used to regenerate the reductant or oxidant of the redox couple.

Borchers was among the first to attempt the construction of a redox fuel cell employing a single redox couple, Cu^{2+}/Cu , in combination with CO as the fuel [4]. The results of Borchers' work, however, were unreliable. Practical and significant progress in the development of redox fuel cells was reported by Posner [5] in England and Carson and Feldman [6] in the United States.

A schematic diagram of a chemically regenerative redox fuel cell is shown in Fig. 1. Posner [5] employed the Br_2/Br^- redox couple as the oxidant and the $\text{Sn}^{2+}/\text{Sn}^{4+}$ redox couple as the reductant. At the anode, electrons are generated by the electrochemical reaction, $\text{Sn}^{2+} \rightarrow \text{Sn}^{4+} + 2e$, and at the cathode electrons are consumed by the electrochemical reaction, $\text{Br}_2 + 2e \rightarrow 2\text{Br}^-$. In his redox cell Posner found the anodic polarization to be quite high, namely 200 mV at 50 mA cm^{-2} current density. The cathodic polarization of the Br_2/Br^- redox couple was very low and seemed to be almost ideal.

Carson and Feldman [6] employed the same oxidant, Br_2 , in the catholyte of their redox cell, but they used a different redox couple, $\text{Ti}^{3+}/\text{TiO}^{2+}$, for their anolyte. The electrode reactions are $\text{Br}_2 + 2e \rightarrow 2\text{Br}^-$ at the cathode, and $\text{Ti}^{3+} + \text{H}_2\text{O} \rightarrow \text{TiO}^{2+} + 2\text{H}^+ + e$ at the anode. They reported an open-circuit voltage (OCV) of 1 V for the redox cell, and at 80 to 85°C this cell delivered 40 mA cm^{-2} at 0.8 V. This is a considerable improvement from Posner's redox fuel cell which had an OCV of 0.8 V and delivered 15 mA cm^{-2} at 0.6 V and 30 mA cm^{-2} at 0.4 V. The power density, which is the product of the voltage and the current density ($\text{V A cm}^{-2} = \text{W cm}^{-2}$), of each cell was too small, and neither of the investigations of these redox systems led to the development of a practical cell.

In spite of the disappointing results from their redox fuel cell work, Posner, and Carson and

Feldman must be given credit for showing the possibility and simplicity of construction and operation of redox fuel cells. Improvements in the performance of redox fuel cells can be achieved in various ways, e.g., by using different redox couples which are known to have high exchange current densities for the redox electrode reactions; by using different electrolytes which are better electrolytic conductors; by using different electrode configurations; by using different electrode materials, and so on. The advantage of the redox fuel cell compared with the direct hydrogen-oxygen or fuel-oxygen cell is that the electrochemical reaction at the electrode is separated from the chemical regeneration reaction, thus circumventing the difficulties associated with the direct-catalysed electrode reactions of gases. This could lead to lower-cost fuel cell electrodes and, as a result, a lower-cost fuel cell system.

2. Experimental

Initial exploratory work on the proposed H_2 - O_2 redox fuel cell consisted of screening candidate redox couples, choosing a supporting electrolyte, membrane and electrode material, as well as designing the cell and its structural arrangement. Candidate redox couples are those couples exhibiting a redox potential close to the hydrogen redox potential [0 V versus the normal hydrogen electrode (NHE)] for the reductant, and a redox potential in the vicinity of the oxygen redox potential (1.23 V versus NHE) for the oxidant. Several of these redox couples are listed in Table 1. This work does not involve the regeneration chemistry.

Experiments employing the $Br_2(l) + 2e \rightarrow 2Br^-$ redox system indicated only a small polarization (50 mV) on the bromine electrode at reasonable current densities (approximately 100 mA cm^{-2}).

This attractive feature of the bromine electrode, however, was overshadowed by the special precautionary measures that must be taken when working with such a hazardous chemical. For the cathodic electrolyte we have worked almost exclusively with the VO_2^+/VO^{2+} system. This system has the advantage of a high voltage, near that of the oxygen electrode, but has the disadvantages of only moderate exchange currents and of difficulty in regeneration [7, 8].

For the anolyte we have worked with Fe^{2+} and Sn^{2+} solutions and with a fixed Cu bed or a slurry of Cu-coated charcoal. The iron and copper systems have high exchange currents whereas Sn^{2+} has only moderate exchange currents [9]. The copper and Sn^{2+} systems have voltages near that of the hydrogen electrode, whereas Fe^{2+} deviates considerably. They can all be regenerated with hydrogen with varying degrees of difficulty [10-14].

Two acidic electrolytes were originally considered: aqueous 45% phosphoric acid (H_3PO_4 ; $k_{max} = 22-23 \Omega^{-1} \text{ m}^{-1}$) and aqueous 30% sulphuric acid (H_2SO_4 ; $k_{max} = 85-87 \Omega^{-1} \text{ m}^{-1}$). The low solubility of V_2O_5 in 45% H_3PO_4 ($6.9 \text{ g dm}^{-3} = 0.038 \text{ M}$) limits the supply of oxidant and thus decreases the usefulness of the phosphoric acid as a supporting electrolyte and solvent. In 30% H_2SO_4 the solubility of V_2O_5 at room temperature was found to be: $25.7 \text{ g dm}^{-3} = 0.14 \text{ M}$.

Commercial cationic exchange membranes, such as Ionic's Nepton 61CZL 183 and IONac MC-3470 and Du Pont's Nafion 427 and 415, were evaluated. Based on its stability in 30% H_2SO_4 , its ease of handling and relatively low electrical resistance, Nafion 415 was selected for the redox fuel cell membrane. Various flow-by electrode configurations were considered: solid graphite, solid porous carbon, a combination of

Table 1. Candidate oxidation-reduction couples for an H_2 - O_2 redox fuel cell in acid solutions

Reductant	E^0 (versus NHE)	Oxidant	E^0 (versus NHE)
$Ti^{3+} + H_2O \rightarrow TiO^{2+} + 2H^+ + e$	-0.1	$VO_2^+ + 2H^+ + e \rightarrow VO^{2+} + H_2O$	1.00
$Sn^{2+} \rightarrow Sn^{4+} + 2e$	-0.15	$Br_2(l) + 2e \rightarrow 2Br^-$	1.065
$Cu^+ \rightarrow Cu^{2+} + e$	-0.153	$Fe^{3+} + e \rightarrow Fe^{2+}$	0.771
$Cu \rightarrow Cu^{2+} + 2e$	-0.337		
$Fe^{2+} \rightarrow Fe^{3+} + e$	-0.771		

Table 2. Properties of VDG carbon felt and WDF graphite felt

Property	VDG carbon felt	WDF graphite felt
Density at 21.1° C (g cm^{-3})	8.33×10^{-2}	8.49×10^{-2}
Water adsorption (at 90% relative humidity) (wt%)	7	0
Surface area ($\text{m}^2 \text{g}^{-1}$)	100	0.5
Amount (g) of 30% H_2SO_4 solution adsorbed per gram of felt:		
as-received	10.5	1.5
after heating at 500° C for 30 min	10.8	14.2
Diameter of fibres in felt (μm)	13	13
Resistivity ($\Omega \text{ cm}$)	4-7	2.1-2.5

a solid graphite current collector with a carbon or graphite felt electrode, or a solid carbon foam with the trade name Reticulated Vitreous Carbon (RVC, Chemtronics International, Ann Arbor, Michigan). The present cell configuration uses a carbon or graphite felt electrode pressed between the membrane separating the catholyte and anolyte and the solid graphite current collector. Two types of felts were used: VDG carbon felt, and WDF graphite felt (Union Carbide). The wetting properties of the felts were determined from the quantity of 30% H_2SO_4 absorbed after 24 hours. From the results shown in Table 2, it is obvious that it is necessary to heat the WDF felt

for 30 min at 500° C before it can be used as an electrode in the redox cell.

The complete redox fuel cell, its components and the recirculation system are illustrated in Fig. 1. Each redox cell consists of two half-cells, made from Teflon or Lexan, separated by a Nafion 415 ion-exchange membrane. Buna rubber or Viton O-rings provide leak-proof, tight seals between each half-cell and the membrane separator. A Masterflex peristaltic pump with Tygon tubing circulates the individual electrolytes through the anode and cathode compartments and returns the electrolyte to the reservoir. The rate of flow can be adjusted from 1.5 to 450 cm^3

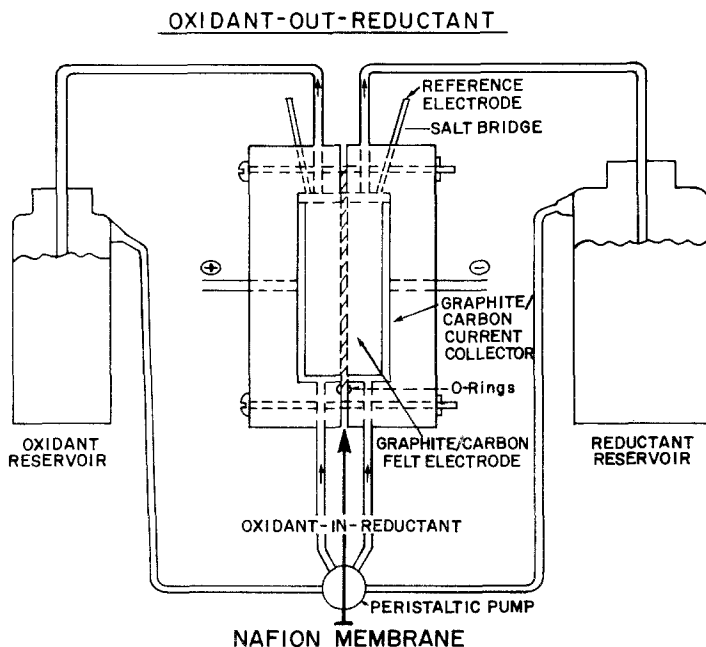


Fig. 1. Regenerative redox fuel cell system.

min^{-1} . Each half-cell is provided with a salt bridge consisting of Teflon tubing filled with a KCl–agar gel and sealed with a glass capillary at one end. This salt bridge is connected to a reference electrode (a saturated KCl/calomel electrode) and is used to record the individual anodic and cathodic potentials of the redox cell. The dimensions of the cell are as follows: outside diameter of each half-cell, 7.65 cm; thickness, 1.19–1.20 cm; electrode compartments, depth = 0.752 cm, diameter = 3.60 cm. The graphite current collectors were made in various thicknesses from 0.20 to 0.46 cm, but with the same circular diameter, 3.17 cm, giving a geometric area of 7.9 cm^2 . More recently other dimensions have been used for the current collectors, namely, a diameter of 3.40 cm, giving a geometric surface area of 9.08 cm^2 .

Discharge curves for these redox cells were obtained by drawing currents through appropriate external resistors of 100, 50, 20, 10, 5, 2, 1 and 0.5 Ω resistance for 4 min and recording the voltages and currents at the end of these four-minute periods. In most cases the observed potentials and currents stabilized after 2 min. The current was read through a Keithley 179–20 A digital multimeter. The total cell voltage and individual cathodic and anodic voltages were recorded on a Varian G4000 and a Hewlett-Packard HP 7100B recorder. An Analogic AN 2570-1-X-1-M digital voltmeter was employed to read the total cell voltage and to calibrate the recorder. The internal resistance of the cell was determined with a Wayne Kerr impedance bridge (Universal Bridge B221 with an Auto-balance Adapter A221 and a Low-Impedance Bridge Adapter Q221A).

During measurements of the internal resistance of the cell and in the experiments for obtaining the voltage versus current densities, it became quite obvious that the use of alligator clips on the graphite rods extending from the current collectors was producing inaccurate results due to poor contact between the alligator clips and the graphite rod. Subsequently the leads were soldered to a copper or brass collar or ring clamp that could be tightly adjusted around the graphite rods. The reservoirs for the reductant and oxidant were immersed in a constant-temperature water bath controlled by a Versa Therm Model

2516 temperature controller. The temperature of the redox fuel cell was monitored by a thermocouple inserted in the current collector. Variations in the temperature were $\pm 0.5^\circ \text{C}$ as indicated by the Doric Trendicator 410A digital temperature indicator for the temperature range 30.0 to 70.0 $^\circ \text{C}$.

3. Results and discussion

The results in this paper pertain to experiments for evaluating the use of various electrode materials and various cell configurations for three redox couples, namely: $\text{VO}_2^+/\text{VO}^{2+}$ – $\text{Sn}^{2+}/\text{Sn}^{4+}$; $\text{VO}_2^+/\text{VO}^{2+}$ – $\text{Fe}^{2+}/\text{Fe}^{3+}$ and $\text{VO}_2^+/\text{VO}^{2+}$ – Cu/Cu^{2+} . Initially, solid porous carbon (PC 59; 200 $\text{m}^2 \text{g}^{-1}$) and graphite were used as electrodes and current collectors with the $\text{VO}_2^+/\text{VO}^{2+}$ – $\text{Sn}^{2+}/\text{Sn}^{4+}$ and $\text{VO}_2^+/\text{VO}^{2+}$ – $\text{Fe}^{2+}/\text{Fe}^{3+}$ systems. The maximum current densities obtained with these electrodes were only of the order of 20–25 mA cm^{-2} at 500 mV discharged through a 1 Ω external resistor. The internal resistance of the redox cell was 0.8 to 1 Ω . A form of rigid carbon foam (Reticulated Vitreous Carbon) was tried as the electrode, with a graphite disc as the current collector. Improvements in the current density (to 50 mA cm^{-2} under similar conditions of discharge) and internal resistance (to 0.6 Ω) were observed. Even higher current densities (100 mA cm^{-2} and higher) and cell voltages were obtained by employing carbon felts (VDG and WDF, Union Carbide) as electrodes in combination with the solid carbon or graphite current collectors. The redox fuel cells that are used to investigate the performance of the various redox systems generally consist of carbon felt electrodes and solid graphite current collectors in each half-cell separated by a Nafion 415 ion-exchange membrane. The use of other electrode materials will be noted accordingly.

3.1. $\text{VO}_2^+/\text{VO}^{2+}$ – $\text{Sn}^{2+}/\text{Sn}^{4+}$ redox cell

One of the advantages of redox fuel cells is that the cell itself (exclusive of regenerators) can, in many cases, be operated near ambient temperatures, thus simplifying the choice of materials for the construction of the cell and its components. The temperature range of operation of the cell is defined by the freezing and boiling point of

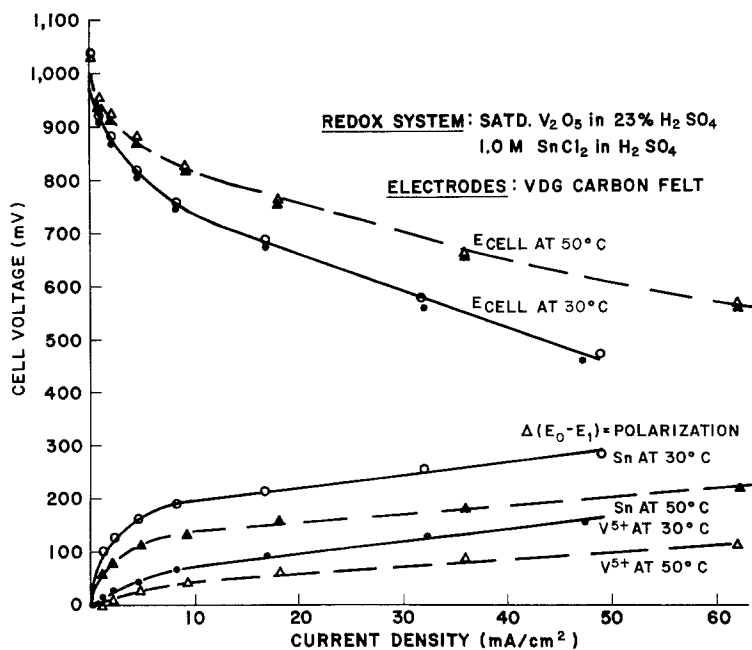


Fig. 2. VO_2^+/VO^{2+} versus Sn^{2+}/Sn^{4+} redox fuel cell performance at $30^\circ C$ and $50^\circ C$.

the supporting electrolyte solution. Raising the temperature of operation above ambient temperature will generally benefit cell performance, because of: (a) the increased solubility of the oxidant and reductant in the supporting electrolyte, (b) an increase in the rate of electrode reactions, and (c) a decrease in the internal resistance. The results from experiments with redox cells operating at 30 and $50^\circ C$ are shown in Fig. 2. At the same current densities (30 and $50 mA cm^{-2}$) the cell voltages are higher at higher temperatures than at lower temperatures, being 700 mV and 610 mV, respectively, at

$50^\circ C$ compared to 590 mV and 450 mV, respectively, at $30^\circ C$. The polarizations $\Delta(E_0 - E_i)$ at the anode (Sn^{2+}/Sn^{4+}) and at the cathode (VO_2^+/VO^{2+}) are lower at the higher temperature.

Although results at $70^\circ C$ showed further improvements in cell performance, for convenience and ease of controlling the thermostatic bath, subsequent experiments with the redox cells were performed at $50.0 \pm 0.5^\circ C$.

Discharge curves for the $VO_2^+/VO^{2+}-Sn^{2+}/Sn^{4+}$ redox cells using VDG carbon felt and WDF graphite felt for the electrodes are shown in Figs. 3 and 4, respectively. The cells using the

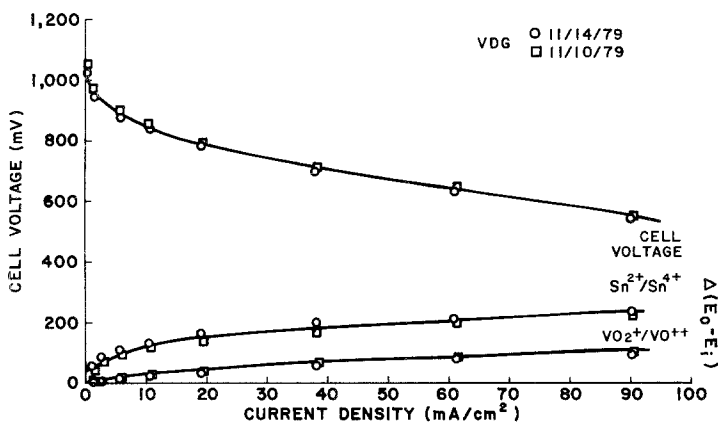


Fig. 3. Performance of VO_2^+/VO^{2+} versus Sn^{2+}/Sn^{4+} redox cell with VDG carbon felt electrodes.

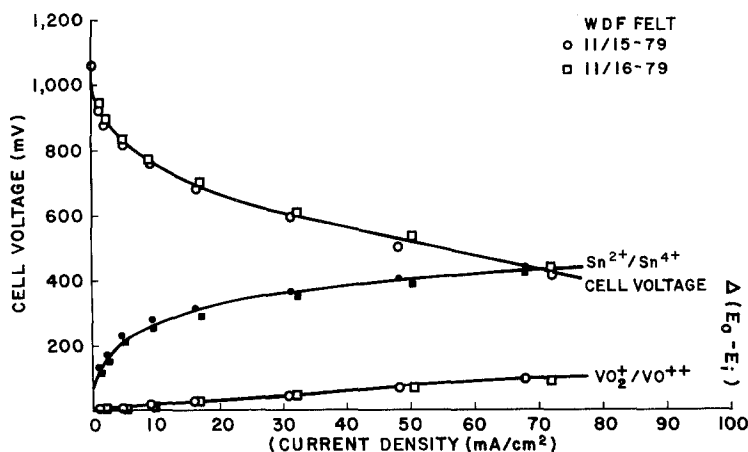


Fig. 4. Performance of $\text{VO}_2^+/\text{VO}^{2+}$ versus $\text{Sn}^{2+}/\text{Sn}^{4+}$ redox cell with WDF carbon felt electrodes.

WDF felt exhibit a considerably higher anodic polarization than the cells using the VDG felt. The difference in electrolyte adsorption by the felts was found to be rather small after the WDF felt was heat-treated at 500°C for 30 min.

The redox reaction, $\text{Sn}^{2+} \rightarrow \text{Sn}^{4+} + 2e$, is known to have a low exchange current density [15] and differences in electrode surface active areas must exert a considerable effect on the polarization of the anode. Thus at the anode, at a current density of 70 mA cm^{-2} , the polarization is approximately 400 mV with the heat-treated WDF felt electrode, compared to approximately 210 mV at the VDG felt electrode. The information supplied by Union Carbide shows that the pristine materials differ considerably in their surface area and water adsorption in 90% relative humidity environment: $100 \text{ m}^2 \text{ g}^{-1}$ and 7 wt% adsorption for the VDG felt and $0.5 \text{ m}^2 \text{ g}^{-1}$ and 0 wt% adsorption for the WDF felt. However, the heat-treated WDF felt (500°C for 30 min) absorbed $14.2 \text{ g } 30\% \text{ H}_2\text{SO}_4$ per gram of felt compared to 10.8 g g^{-1} VDG felt. Thus, although the heat treatment of the WDF felt has considerably improved its ability to absorb the aqueous electrolyte, the high polarization of the $\text{Sn}^{2+}/\text{Sn}^{4+}$ electrode is an indication that it has less surface activity than the VDG felt.

The polarization on the cathodic side ($\text{VO}_2^+/\text{VO}^{2+}$) was comparatively low, approximately 125–130 mV at a current density of 70 mA cm^{-2} , and independent of the felt. Discharging through a 0.5Ω resistor, the maximum power density of the cell with the WDF felt was $0.45 \times 0.74 \text{ W cm}^{-2} =$

0.033 W cm^{-2} ($= 30.9 \text{ W ft}^{-2}$), and with the VDG felt, $0.55 \times 0.09 = 0.0495 \text{ W cm}^{-2}$ (46 W ft^{-2}).

In our attempts to further improve the performance of the cathode, ionic compounds that were known to promote redox reactions (e.g. Pd^{2+} , Mn^{2+} , Fe^{3+} -phenanthroline, U^{4+} , Ag^+ and Hg^{2+}) were added in small quantities to the catholyte (saturated V_2O_5 solution in 30% H_2SO_4). None of these species were found to affect the magnitude of the polarization at the cathode. Addition of 1 cm^3 0.2 N Br_2 solution in 30% H_2SO_4 seemed to lower the polarization at the cathode by approximately 25–30 mV, and therefore could be considered for future redox cell improvements.

Another approach for improving the redox cell performance is to disperse a metal into the felt in an attempt to catalyse the anodic reaction $\text{Sn}^{2+} \rightarrow \text{Sn}^{4+} + 2e$ [16]. Among the metals (Cu, Ni, Au and Pt) that were tried, only the Pt dispersion seemed to be effective. The discharge curves of the redox cells employing VDG and WDF felt with various loadings of Pt and without Pt are shown in Figs. 5 and 6, respectively. Besides the cell voltage versus current density, only the anodic polarization $\Delta(E_0 - E_i)$ versus current density is plotted on the graphs. The anodic polarization at the platinized felts drops considerably, particularly in the case of the WDF felt, from approximately 400 mV (by extrapolation) to approximately 150 mV at 120 mA cm^{-2} current density. The VDG felt showed a polarization of approximately 250 mV without Pt and only 150 mV with Pt.

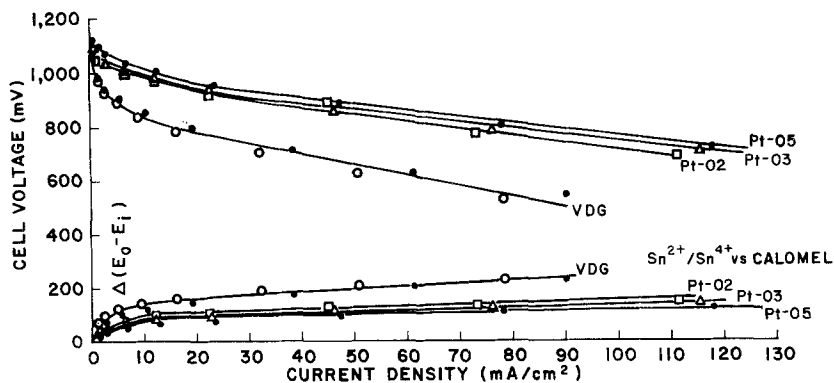


Fig. 5. Effect of Pt Impregnation of VDG carbon felt on the performance of a $\text{VO}_2^+/\text{VO}^{2+}$ versus $\text{Sn}^{2+}/\text{Sn}^{4+}$ redox cell.

This reduction in the anodic polarization leads to overall improvement of cell performance, as is shown by the power output of the redox cells at a current density of 110 mA cm^{-2} (see Table 3).

At present it is premature to draw any conclusions on the relation between the loading of the felt and the power density of the cell based upon this limited amount of experimentation. Although the gain in power output is substantial in comparison with the unplatinized felt electrodes ($0.033 \text{ W cm}^{-2} = 30.9 \text{ W ft}^{-2}$ with the WDF felt and $0.049 \text{ W cm}^{-2} = 46 \text{ W ft}^{-2}$ with the VDG felt), it is economically unjustifiable to use Pt in a practical cell. These experiments indicate that if a suitable inexpensive catalyst can be found to lower the polarization on the $\text{Sn}^{2+}/\text{Sn}^{4+}$ anode it

is possible to improve the cell performance of the $\text{VO}_2^+/\text{VO}^{2+}-\text{Sn}^{2+}/\text{Sn}^{4+}$ redox cell to such an extent that the cell itself (exclusive of regenerators) will present a feasible alternative to the conventional fuel cell.

3.2. $\text{VO}_2^+/\text{VO}^{2+}-\text{Fe}^{2+}/\text{Fe}^{3+}$ cell

The redox couple $\text{Fe}^{2+}/\text{Fe}^{3+}$ is a potential alternative to the $\text{Sn}^{2+}/\text{Sn}^{4+}$ couple since it has a much higher exchange current density (10 to 1000 times higher) [9]. One drawback is the fact that it has a rather high redox potential of 0.7 V versus the normal hydrogen electrode. It is well known, however, that in different media, due to complexation, solvation, etc., the redox potential can change

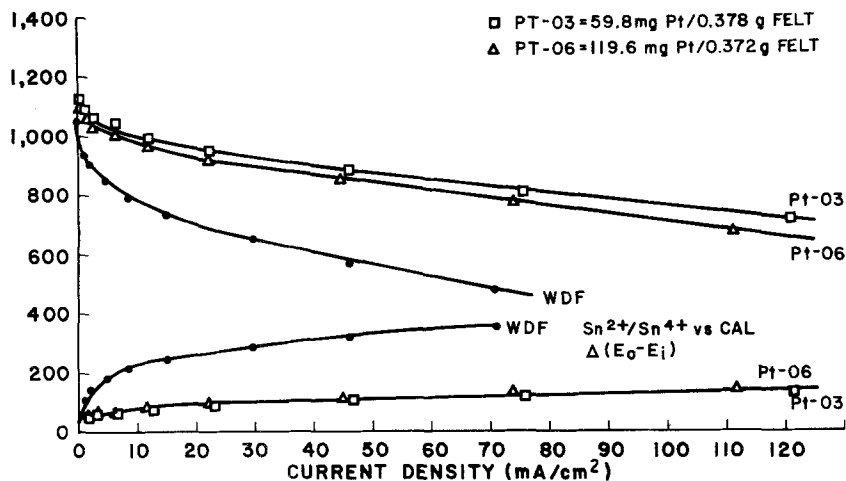


Fig. 6. Effect of Pt impregnation of WDF carbon felt on the performance of a $\text{VO}_2^+/\text{VO}^{2+}$ versus $\text{Sn}^{2+}/\text{Sn}^{4+}$ redox cell.

Table 3. Variation of power density from cell with amount of platinum in felt

Electrode	Platinum in felt (mg)	Power density (W cm^{-2})
VDG-PT-05	119.6	$0.75 \times 0.11 = 0.083$ (76.6) [†]
VDG-PT-03	59.8	$0.725 \times 0.11 = 0.080$ (74.1)
VDG-PT-02	29.9	$0.685 \times 0.11 = 0.075$ (70.0)
WDF-PT-06	119.6	$0.678 \times 0.11 = 0.075$ (70.0)
WDF-PT-03	53.8	$0.74 \times 0.11 = 0.081$ (75.6)

[†] Values in parentheses give power density in W ft^{-2} .

considerably. For example, in 4 M phosphoric acid, the formal redox potential of the $\text{Fe}^{2+}/\text{Fe}^{3+}$ couple decreases to 0.46 V. Similarly in 30% H_2SO_4 the redox potential versus the saturated calomel reference electrode is found to be 0.26–0.28 V, which corresponds to a value of 0.54–0.56 V versus the normal hydrogen electrode. Discharge curves and polarization curves for the anode and cathode of $\text{VO}_2^+/\text{VO}^{2+}-\text{Fe}^{2+}/\text{Fe}^{3+}$ redox cells are shown in Fig. 7. The difference in the cell performance of the two cells with the WDF and VDG felts is rather small and well within the limits of experimental error. The polarization curves for the anode and cathode are almost identical. At a current density of 90 mA cm^{-2} the polarization of the $\text{Fe}^{2+}/\text{Fe}^{3+}$ electrode amounts to only 50 mV, less than half of the polarization at the $\text{VO}_2^+/\text{VO}^{2+}$ electrode (approximately 120 mV).

At the above current density (90 mA cm^{-2}), the power densities of the cells are: $0.5 \times 0.09 \text{ W cm}^{-2} = 0.045 \text{ W cm}^{-2}$ (42 W ft^{-2}) for the VDG electrodes and $0.54 \times 0.09 = 0.049 \text{ W cm}^{-2}$ (45 W ft^{-2}) for the WDF electrodes. This is comparable to the power density of the previously

described $\text{VO}_2^+/\text{VO}^{2+}-\text{Sn}^{2+}/\text{Sn}^{4+}$ redox fuel cell. This power density is low.

3.3. $\text{VO}_2^+/\text{VO}^{2+}-\text{Cu}/\text{Cu}^{2+}$ redox cell

Copper can be easily oxidized in sulphuric acid solutions to Cu^{2+} and the exchange current density reported for the reaction, $\text{Cu} \rightarrow \text{Cu}^{2+} + 2e$ in 2 N H_2SO_4 , is of the order of $2 \times 10^{-2} \text{ A cm}^{-2}$ [17], considerably higher than the exchange current density for the $\text{Sn}^{2+}/\text{Sn}^{4+}$ redox couple. The normal redox potential of the copper/cupric couple is 0.34 V, approximately 0.4 V lower than for the ferrous/ferric couple. Therefore, it can be expected that the cell voltage of this redox cell will be higher than for the $\text{VO}_2^+/\text{VO}^{2+}-\text{Fe}^{2+}/\text{Fe}^{3+}$ redox cell.

In the anodic reaction, copper is consumed, thus the anode current collector must not contain Cu as this will be gradually dissolved during the operation of the redox cell. Copper must thus be part of the anolyte and be supplied continuously to the anode. Efforts to use a Cu dispersion in the 30% H_2SO_4 supporting electrolyte have thus far

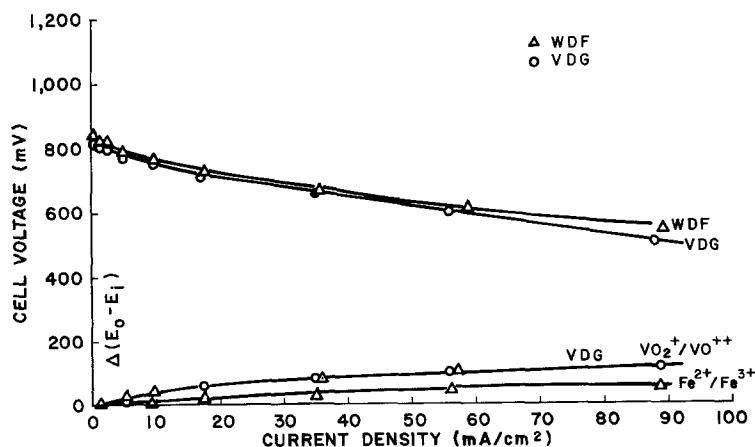


Fig. 7. Performance of $\text{VO}_2^+/\text{VO}^{2+}$ versus $\text{Fe}^{2+}/\text{Fe}^{3+}$ redox cell.

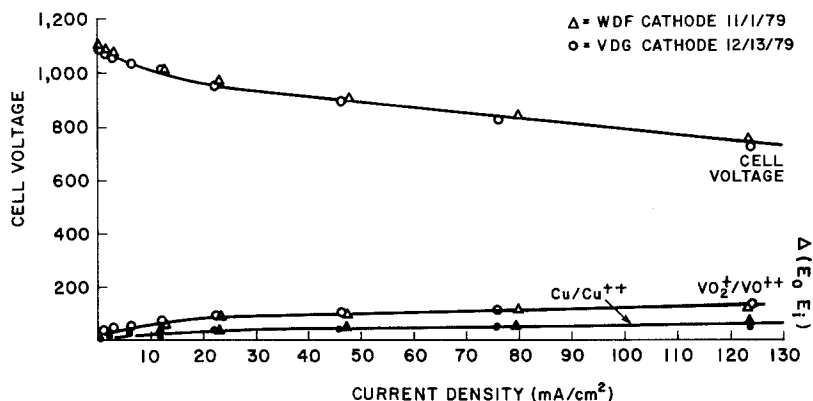


Fig. 8. Performance of $\text{VO}_2^+/\text{VO}^{2+}$ versus Cu/Cu^{2+} redox cell.

been unsuccessful. The redox cells that were used to evaluate the Cu/Cu^{2+} couple consisted of the usual solid graphite current collector and a VDG felt electrode for the cathode and a Cu -wool disc for the anode. The results of some of these experiments are shown in Fig. 8. The redox cells based on the $\text{VO}_2^+/\text{VO}^{2+}$ - Cu/Cu^{2+} couples have consistently shown good overall performance with a cell voltage of 0.75 V at 124 mA cm^{-2} , corresponding to a power density of $0.75 \times 124 \text{ W cm}^{-2} = 0.093 \text{ W cm}^{-2}$ (86 W ft^{-2}). The experimental conditions and configurations consisted of: a catholyte of a saturated solution of V_2O_5 in 30% H_2SO_4 ; a VDG felt cathode pressed between a Nafion 415 membrane and a graphite current collector; an anolyte of 30% $\text{H}_2\text{SO}_4 + 10 \text{ cm}^3 10^{-2} \text{ M CuSO}_4$ solution; a Cu -wool disc pressed between the membrane and the graphite current collector and a cell temperature of $50.0 \pm 0.5^\circ \text{C}$.

The high exchange current density for the electron exchange reaction, $\text{Cu} \rightarrow \text{Cu}^{2+} + 2e$, is reflected in the low polarization (less than 60 mV at 124 mA cm^{-2}) of the anode. The polarization at the cathode remained above 100 mV (approximately 115–125 mV). The internal resistance of the cell was found to be around 0.1Ω . Considering the present performance achievement of the $\text{VO}_2^+/\text{VO}^{2+}$ - Cu/Cu^{2+} redox cell, only minor improvements are necessary to attain a performance goal of 0.75 V at 200 mA cm^{-2} for this redox cell. This corresponds to a power density of 0.15 W cm^{-2} (139 W ft^{-2}). Although this goal for the electrochemical performance of the cell should be within reach of our current efforts, the feasibility of the complete redox cell depends on other important factors, including the regeneration chemistry of the oxidant and reductant and the possibility of using slurry electrolytes. Exploratory experiments

Table 4. $\text{VO}_2^+/\text{VO}^{2+}$ - Cu/Cu^{2+} cell performance

External load (Ω)	Cell voltage (mV)	Current density (mA cm^{-2})	Cathode		Anode	
			Voltage (mV)	Polarization (mV)	Voltage (mV)	Polarization (mV)
∞	890	0	930	0	40	0
100	845	0.96	896	34	41	1
50	816	1.8	863	67	43	3
20	771	4.3	826	104	45	5
10	727	7.8	795	135	48	8
5	668	13.9	757	173	54	14
2	560	25.9	700	230	70	30
1	456	37.2	650	280	90	50
0.5	338	50.6	600	330	130	90

with an anodic slurry electrolyte consisting of 500 cm³ of 30% H₂SO₄ containing 200 g charcoal (< 125 μm) on which 0.25 M Cu was electrolessly deposited, showed that such a cell in combination with a VO₂⁺/VO²⁺ cathode gave promising results. The results of such an experiment are shown in Table 4.

The felt electrode in this cell was replaced by a porous Reticulated Vitreous Carbon electrode to accommodate the flow of the slurry. The accompanying loss in cell conductance resulted in lower overall cell performance. Nevertheless, the results showed that within the severe constraints of the experiments, such as low Cu concentration and non-optimized electrode structure, it is possible to construct a VO₂⁺/VO²⁺-Cu/Cu²⁺ redox fuel cell using an anodic slurry electrolyte of Cu on charcoal. The use of a copper slurry could be compatible with the regeneration of cupric sulphate solutions with H₂ [12-14].

4. Conclusion

Exploratory experiments with three types of redox fuel cells utilizing the couples VO₂⁺/VO²⁺-Sn²⁺/Sn⁴⁺, VO₂⁺/VO²⁺-Fe²⁺/Fe³⁺ and VO₂⁺/VO²⁺-Cu/Cu²⁺ have shown the potential features and some of the problems in the discharge operation of redox fuel cells. The results show that large electrode polarization (150 mV) resulting in power density losses can be avoided in two ways: (a) by catalysing the electrode reaction, such as in the case of the Sn²⁺/Sn⁴⁺ electrode where activation polarization is the main problem, and (b) by maximizing the surface/volume ratio of the electrode material and thus minimizing any mass-transfer problems. In order to achieve a high power density, the choice of anodic and cathodic redox couples is limited to those couples with a reasonably high exchange current density (preferably of the uncatalysed redox reaction) and whose redox potentials are in the vicinity of the hydrogen and oxygen redox potentials (0 and 1.23 V respectively).

The VO₂⁺/VO²⁺-Cu/Cu²⁺ redox fuel cell exemplifies the previous statement. Even in these exploratory experiments, without any special effort to optimize the cell and electrode configuration for maximum performance, this cell achieved a power density of 0.095 W cm⁻² (86 W ft⁻²). It

can be expected that, with some modification in the cell and electrode configuration to promote better electrolyte/electrode contact and to decrease the internal cell resistance, an improvement in cell performance can be attained and a power density of 0.75 V × 0.20 = 0.15 W cm⁻² (139 W ft⁻²) can be achieved.

The redox couples that were studied in this report can all be chemically regenerated with H₂ and O₂. Thus the redox fuel cells utilizing these redox couples are chemically regenerative redox fuel cells and are distinct from other studied and reported redox fuel cells which are electrically regenerated [18, 19]. These electrically regenerated redox fuel cells are essentially secondary batteries.

References

- [1] W. Vielstich, 'Brennstoffelemente', Verlag Chemie, Weinheim, West Germany (1965).
- [2] K. R. Williams (editor), 'An Introduction to Fuel Cells', Elsevier, Amsterdam (1966).
- [3] E. W. Justi and A. W. Winsel, 'Kalte Verbrennung' ('Fuel Cells'), Franz Stein Verlag, Wiesbaden, West Germany (1962).
- [4] J. M. Matsen, in 'Regenerative EMF Cells', (edited by R. F. Gould) *Advanced Chemistry Series*, Vol. 64, American Chemical Society, Washington, DC (1967).
- [5] A. M. Posner, *Fuels* 24 (1955) 330.
- [6] W. M. Carson and M. L. Feldman, *Proc. 13th Annual Power Sources Conf.*, Fort Monmouth, New Jersey (1959).
- [7] K. Post, PhD Dissertation, University of New South Wales, Kensington, Australia (1976).
- [8] M. Kranz, 'Oxidation of VOSO₄ in the Presence of Small Amounts of Other Materials', *CA* 55, 5216 f (1961).
- [9] R. O. Miller, 'Electrochemical Behavior of 0.2 to 3 Ferrous Chloride-Ferric Chloride Mixtures on Edge-on Pyrolytic Graphite Rotated Disk Electrode', ERDA/NASA-5022/77/2, NASA Report TM-73716 (1977).
- [10] D. Horvitz, 'Stannic Halide Solution Reduction with H₂', US Patent 3053 621, CA 161341 (1962).
- [11] J. Benard and P. Albert, *Compt. Rend. Acad. Sci. Paris* 224 (1947) 45.
- [12] B. Meddings and V. N. Mackiw, in 'Unit Processes in Hydrometallurgy' (edited by M. E. Wadsworth and F. T. Davis) Gordon and Breach, New York (1965).
- [13] E. Peters and E. A. von Hahn, in 'Unit Processes in Hydrometallurgy' (edited by M. E. Wadsworth and F. T. Davis) Gordon and Breach, New York (1965) p. 204.
- [14] E. A. von Hahn and E. Peters, *J. Phys. Chem.* 69 (1965) 547.
- [15] J. Giner, 'Screening of Redox Couples and Elec-

-
- trode Materials', NASA Report CR-134 705 (1976).
- [16] A. P. Bond and D. Singman, 'Electrode Kinetics of Oxidation-Reduction Couples', DOFL Report No. TR-835, PB-146398 (1960).
- [17] T. Erdey-Gruz, 'Kinetics of Electrode Processes', Wiley-Interscience, New York (1972) p. 320.
- [18] R. S. Yeo, J. McBreen, A. A. C. Tseung and S. Srinivasan, *J. Appl. Electrochem.* **10** (1980) 393.
- [19] L. H. Thaller, 'Redox Flow Cell Energy Storage Systems', NASA TM-79143, DOE/NASA/1002-79/3 (1979).